
CoSP: Co-supervised pretraining of pocket and ligand

Zhangyang Gao

Cheng Tan

Lirong Wu

Stan Z. Li *

Abstract

Can we inject the pocket-ligand interaction knowledge into the pre-trained model and jointly learn their chemical space? Pretraining molecules and proteins has attracted considerable attention in recent years, while most of these approaches focus on learning one of the chemical spaces and lack the injection of biological knowledge. We propose a co-supervised pretraining (CoSP) framework to simultaneously learn 3D pocket and ligand representations. We use a gated geometric message passing layer to model both 3D pockets and ligands, where each node’s chemical features, geometric position and orientation are considered. To learn biological meaningful embeddings, we inject the pocket-ligand interaction knowledge into the pretraining model via contrastive loss. Considering the specificity of molecules, we further propose a chemical similarity-enhanced negative sampling strategy to improve the contrastive learning performance. Through extensive experiments, we conclude that CoSP can achieve competitive results in pocket matching, molecule property predictions, and virtual screening.

1 Introduction

Is there a pretrained model that explores the chemical space of pockets and ligands while considering their interactions? Recently, many deep learning methods have been proposed to understand the chemical space of protein pockets or drug molecules (or called ligands) and facilitate drug design in many aspects, e.g., finding hits for a novel target [50], repurposing ancient drugs for new targets [20, 48, 58], and searching for similar pockets and molecules [29, 39]. While deep learning models have shown promising potential in learning separate pocket space or molecular space for specific tasks [14, 17, 25, 40, 61], jointly pretrain pockets and ligands considering their interactions, rather than learning the pocket or molecular spaces individually, remains to be explored.

We propose **co-supervised pretraining** (CoSP) framework for understanding the joint chemical space of pockets and ligands. Taking the ligand as an example, contrastive self-supervised pretraining [14, 42, 47] has attracted considerable attention and yielded significant achievements in recent years. By identifying expertly defined positive and negative ligand pairs, the model can learn the underlying knowledge to facilitate downstream tasks. However, most self-supervised methods capture data dependencies in the "self" data domain while ignoring additional information from other complementary fields, such as bindable pockets. To fill this knowledge gap, we introduce cross-domain dependencies between pockets and ligands to optimize the representations. The basic assumption is that functionally similar molecules prefer to bind to similar pockets and vice versa.

We propose **gated geometric message passing** (GGMP) layer to extract expressive bio-representations for 3D pockets and ligands. All bio-objects are treated as 3D graphs in that each node contains invariant chemical features (atomic number, etc.) and equivalent geometric features (position and direction). For each bio-object, we analyze the pairwise energy function [18], which considers both chemical features and geometric features via the gated operation. By minimizing the energy function, we derive the updating rules of position and direction vectors. Finally, we combine these rules with classical message passing, resulting in GGMP.

We introduce ChemInfoNCE loss to reduce the negative sampling bias. When applying contrastive learning, the false negative pairs that are actually positive will lead to performance degradation, called negative sampling bias. Chuang et al. [7] assume that the label distribution of the classification task is uniform and propose Debiased InfoNCE to alleviate this problem. Considering the specificity of the molecules and extending the situation to continuous properties prediction (regression task), we propose the chemical similarity-enhanced negative ligand sampling strategy. Interestingly, the change in sampling is equivalent to the change in the sample weights. From the view of loss functions, we provide a systematic understanding and propose ChemInfoNCE.

We evaluate our model on several downstream tasks, from pocket matching, molecule property prediction to virtual screening. Numerous experiments show that our approach can achieve competitive results on these tasks, which may provide a good start for future AI drug discovery.

2 Related work

Motivation Protein and molecule show their biological functions by binding with each other [5], thus exploring the protein-ligand complex help to improve the understanding of both proteins, molecules, and their interactions. To improve the generalization ability and reduce the complexity, we further consider local patterns about the protein pocket x and its ligand \hat{x} . Taking (x, \hat{x}) as the positive pair, while (x, \hat{x}^-) as the negative pair, where \hat{x}^- could not bind to x , we aim to pretrain pocket model $f : x \mapsto \mathbf{h}$ and a ligand model $\hat{f} : \hat{x} \mapsto \hat{\mathbf{h}}$, such that the mutual information between \mathbf{h} and $\hat{\mathbf{h}}$ will be maximized.

Equivalent 3D GNN Extensive works have shown that 3D structural conformation can improve the quality of bio-representations with the help of equivalent message passing layer [3, 4, 8, 15, 34, 43]. Inspired by the energy analysis [16, 18], we propose a new **g**ated **g**eometric **m**essage **p**assing (GGMP) layer that consider not only the node position but also its direction, where the latter could indicate the cavity position of the pocket and describe the 3D rotational state.

InfoNCE The original InfoNCE is proposed by [30] to contrast semantically similar (positive) and dissimilar (negative) pairs of data points, such that the representations of similar pairs (x, \hat{x}) to be close, and those of dissimilar pairs (x, \hat{x}^-) to be more orthogonal. By default, the negative pairs are uniformly sampled from the data distribution. Therefore, false negative pairs will lead to significant performance drop. To address this issue, DebiasedInfoNCE[7] is proposed, which assumes that the label distribution of the classification task is uniform. Although DebiasedInfoNCE has achieved good results on image classification, it is not suitable for direct transfer to regression tasks, and the uniform distribution assumption may be too strict. As to the bio-objects, we discard the above assumption, extend the situation to continuous attribute prediction, use fingerprint similarity to measure the probability of negative ligands, and propose ChemInfoNCE.

Self Bio-Pretraining Many pre-training methods have been proposed for a single protein or ligand single domain, which can be classified as sequence-based, graph-based or structure-based. We summarize the **protein pretraining** models in Table.1. As for sequential models, CPCPort [27] maximizes the mutual information between predicted residues and context. Profile Prediction [41] suggests predicting MSA profile as a new pretraining task. OntoProtein [60] integrates GO (Gene Ontology) knowledge graphs into protein pre-training. While most of the sequence models rely on the transformer architecture, CARP [57] finds that CNNs can achieve competitive results with much fewer parameters and runtime costs. Recently, GearNet [64] explores the potential of 3D structural pre-training from the perspective of masked prediction and contrastive learning. We also summarize the **molecule pretraining** models in Table.1. As for sequential models, FragNet [37] combines masked language model and multi-view contrastive learning to maximize the inner mutual information of the same SMILES and the agreement across augmented SMILES. Beyond SMILES, more approaches [14, 23, 33, 42, 47, 61, 63] tend to choose graph representation that can better model structural information. For example, Grover [33] integrates message passing and transformer architectures and pre-trains a super-large GNN using 10 million molecules. MICRO-Graph [61] and MGSSL [63] use motifs for contrastive learning. Considering the domain knowledge, MoCL [42] uses substructure substitution as a new data augmentation operation and predicts pairwise fingerprint similarities. Although these pre-training methods show promising results, they do not consider

the 3D molecular conformations. To fill this gap, GraphMVP [25] and 3DInfomax [40] explore to maximize the mutual information between 3D and 2D views of the same molecule and achieve further performance improvements. Besides, GEM [13] proposes a geometry-enhanced graph neural network and pretrains it via geometric tasks. For the pretraining of individual proteins or molecules, these methods demonstrate promising potential on various downstream tasks but ignore their interactions.

Method	Protein Data	Code	Year	Method	Molecule Data	Code	Year
CPCProt [27]	sequence	PyTorch	2020	FragNet [37]	SMILES	–	2021
Profile Prediction [41]	sequence	–	2020	MoCL [42]	graph	PyTorch	2021
ONTOPROTEIN [60]	sequence	PyTorch	2022	MPG [23]	graph	PyTorch	2021
CARP	sequence	–	2022	Grover [33]	graph	PyTorch	2020
GearNet	3D	–	2022	MICRO-Graph [61]	graph	–	2020
				CKGNN [14]	graph	–	2021
				MGSSL [63]	graph	PyTorch	2021
				MolCLR [47]	graph	PyTorch	2022
				3DInfomax [40]	graph+3D	PyTorch	2021
				GraphMVP [25]	graph+3D	–	2022
				GEM [13]	graph+3D	Paddle	2022

Table 1: Protein and molecule pretraining methods

Cross Bio-Pretraining In parallel with our study, Uni-Mol [65], probably the first pretrained model that can handle both protein pockets and molecules, released the preprinted version. Compared with them, our approach differs in pretrained data, pretraining strategy, model architecture, and downstream tasks.

3 Methodology

3.1 Co-supervised pretraining framework

We propose the **co-supervised pretraining (CoSP)** framework, as shown in Figure.1, to explore the joint chemical space of protein pockets and ligands, where the methodological innovations include:

- We propose the gated geometric message passing layer to model 3D pockets and ligands.
- We propose a co-supervised pretraining framework to learn pocket and ligand representations.
- We propose ChemInfoNCE with improved negative sampling guided by chemical knowledge.
- We evaluate the pretrained model on both pocket matching, molecule property prediction, and virtual-screening tasks.

3.2 Geometric Representation

We introduce the unified data representation and neural network for modeling 3D pockets and ligands. All structures used for pre-training are collected from the BioLip dataset. In downstream tasks where ligand conformations are not provided, we generate 3D conformations using MMFF (if successful) or their 2D conformations (if failed).

Pocket and Ligand Graph We represent bio-object as graph $\mathcal{G}(X, \mathcal{V}, \mathcal{E})$, consisting of coordinate matrix $X \in \mathbb{R}^{n,3}$, node features $\mathcal{V} \in \mathbb{R}^{n,d_f}$, and edge features $\mathcal{E} \in \mathbb{R}^{n,d_e}$. For pockets, the graph nodes include amino acids within 10\AA to the ligand, X contains the position of C_α of residues, on which we construct \mathcal{E} via k-nn algorithm. For molecules, the graph nodes include all ligand atoms except Hs, X contains the atom positions, and we use the molecular bonds as \mathcal{E} .

Gated Geometric Message Passing From layer t to $t+1$, we use the gated geometric message passing (GGMP) layer to update 3D graph representations, i.e., $[v_i^{t+1}, x_i^{t+1}, n_i^{t+1}] = \text{GGMP}(v_i^t, x_i^t, n_i^t)$, where n_i is the direction vector that point to the neighborhood center of node i . For protein pockets,

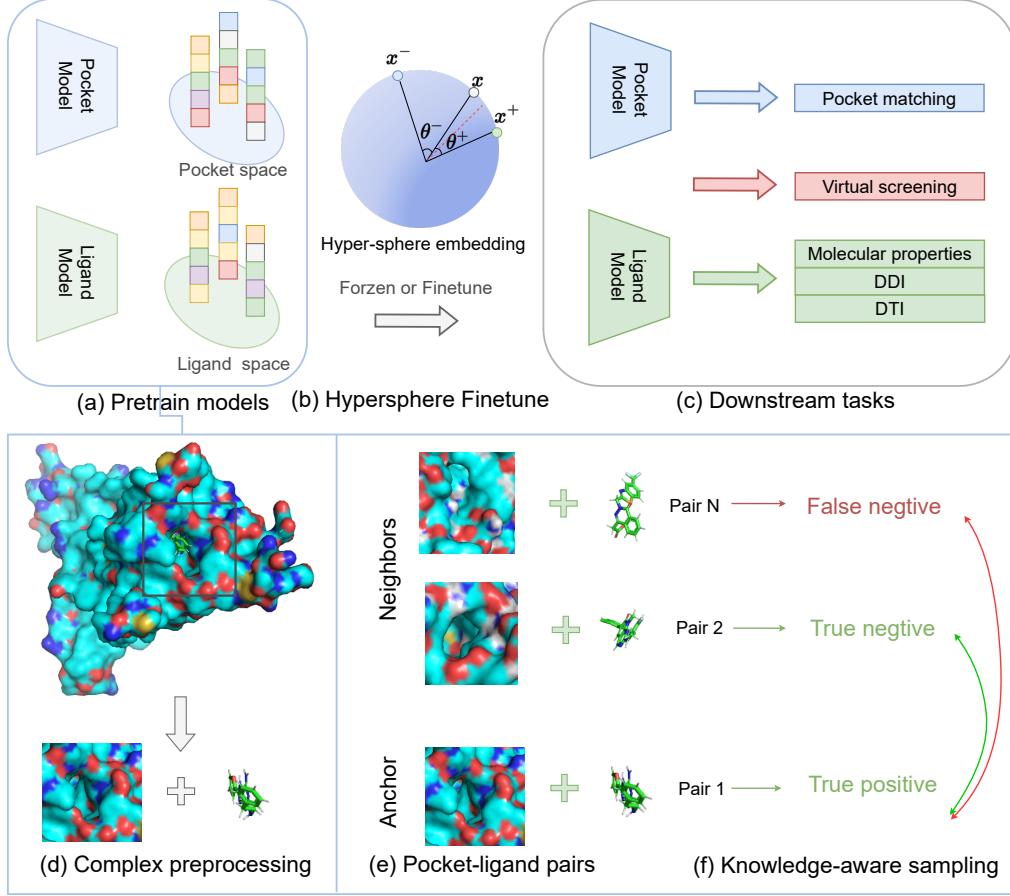


Figure 1: Overview of CoSP. We contrast bound pocket-ligand pairs with unbound ones to learn the interaction-aware chemical embeddings.

\mathbf{n}_i could indicate the position of protein caves. As to the 3D conformations, we minimize the pairwise energy function $E(X, F, \mathcal{E})$:

$$E(X, F, \mathcal{E}) = \sum_{(i,j) \in \mathcal{E}} u(\mathbf{v}_i, \mathbf{v}_j, \mathbf{e}_{ij}) g(\langle \mathbf{n}_i, \mathbf{n}_j \rangle, d_{ij}^2) \quad (1)$$

where $d_{ij}^2 = \|\mathbf{x}_i - \mathbf{x}_j\|^2$, both chemical energy $u(\cdot)$ and geometric energy $g(\cdot)$ are considered. By calculating the gradients of \mathbf{x}_i and \mathbf{n}_i , we get their updating rules:

$$-\frac{\partial E(X, F, \mathcal{E})}{\partial \mathbf{x}_i} = -\sum_{j \in \mathcal{N}_i} 2u_{ij} \frac{\partial g_{ij}}{\partial d_{ij}^2} (\mathbf{x}_i - \mathbf{x}_j) \approx \sum_{j \in \mathcal{N}_i} u(\mathbf{v}_i, \mathbf{v}_j, \mathbf{e}_{ij}) \phi_x(d_{ij}^2, \langle \mathbf{n}_i^t, \mathbf{n}_j^t \rangle) (\mathbf{x}_i^t - \mathbf{x}_j^t) \quad (2)$$

$$-\frac{\partial E(X, F, \mathcal{E})}{\partial \mathbf{n}_i} = -\sum_{j \in \mathcal{N}_i} u_{ij} \frac{\partial g_{ij}}{\partial \langle \mathbf{n}_i, \mathbf{n}_j \rangle} \mathbf{n}_j \approx \sum_{j \in \mathcal{N}_i} u(\mathbf{v}_i, \mathbf{v}_j, \mathbf{e}_{ij}) \phi_n(d_{ij}^2, \langle \mathbf{n}_i^t, \mathbf{n}_j^t \rangle) \mathbf{n}_j^t \quad (3)$$

$$(4)$$

Note that ϕ_x and ϕ_n are the approximation of $\frac{\partial g_{ij}}{\partial d_{ij}^2}$ and $\frac{\partial g_{ij}}{\partial \langle \mathbf{n}_i, \mathbf{n}_j \rangle}$. Combining graph message passing, we propose the GGMP:

$$\mathbf{m}_{ij} = \phi_m(\mathbf{v}_i^t, \mathbf{v}_j^t, e_{ij}) \quad (5)$$

$$\mathbf{g}_{ij} = \phi_g(d_{ij}^2, \langle \mathbf{n}_i^t, \mathbf{n}_j^t \rangle) \quad (6)$$

$$\mathbf{h}_i^{t+1} = \phi_h(\mathbf{h}_i^t, \sum_{j \in \mathcal{N}_i} \mathbf{m}_{ij} \mathbf{g}_{ij}) \quad (7)$$

$$\mathbf{x}_i^{t+1} = \mathbf{x}_i^t + \lambda \sum_{j \in \mathcal{N}_i} u(\mathbf{m}_{ij}) \phi_x(\mathbf{g}_{ij})(\mathbf{x}_i^t - \mathbf{x}_j^t) \quad (8)$$

$$\mathbf{n}_i^{t+1} = \mathbf{n}_i^t + \lambda \sum_{j \in \mathcal{N}_i} u(\mathbf{m}_{ij}) \phi_n(\mathbf{g}_{ij}) \mathbf{n}_j^t \quad (9)$$

$$(10)$$

where ϕ_* and u are approximated by neural networks. As suggested in [16, 18], the neural layer could learn expressive representations by considering both geometric constraints and chemical features.

3.3 Contrastive loss

In contrastive learning, the biased negative sampling could impair the performance, in which case false negative pairs are sampled for training. Previous methods [7, 32] address this problem by simply considering the class distribution of false-negative samples as uniform under the classification setting. We propose chemical knowledge-based sampling to better address this issue, where fingerprint similarity is used to measure the probability of negative ligands. Interestingly, the change in sampling distribution is actually equivalent to the design of a weighted loss, and we provide a comprehensive understanding from the perspective of contrastive loss.

Uni-contrastive loss Given the pocket $x \sim p$, we draw positive ligands \hat{x}^+ from the distribution \hat{p}_x^+ of bindable molecules and negative ligands $\{\hat{x}_i^-\}_{i=1}^N$ from the distribution \hat{q} of non-bindable ones. By default, the positive ligands are determined by the pocket-ligand complexes, while negative are uniformly sampled from the ligand sets. We use pocket model f and ligand model \hat{f} to pockets and ligands into the latent space, resulting in $\mathbf{h}, \hat{\mathbf{h}}^+$ and $\{\hat{\mathbf{h}}_i^-\}_{i=1}^N$, and maximize the positive similarity $s^+ = \text{sim}(\mathbf{h}, \hat{\mathbf{h}})$ against the negative similarities $s_i^- = \text{sim}(\mathbf{h}, \hat{\mathbf{h}}_i^-), i = 1, 2, \dots$, resulting in:

$$L_{\text{Uni}} = \mathbb{E}_{\substack{x \sim p, \hat{x}^+ \sim \hat{p}_x^+, \\ \{\hat{x}_i^-\}_{i=1}^N \sim \hat{q}}} \left[\log \left(1 + \frac{Q}{N} \sum_{i=1}^N s_i^- / s^+ \right) \right] \quad (11)$$

$$(12)$$

For each data sample x , the gradients contributed to s^+ and s_i^- are:

$$\frac{\partial L}{\partial s^+} = \frac{1}{1 + \sum_{i=1}^N s_i^- / s^+} \sum_{i=1}^N \frac{\partial s_i^- / s^+}{\partial s^+} \quad (13)$$

$$\frac{\partial L}{\partial s_i^-} = \frac{1}{1 + \sum_{i=1}^N s_i^- / s^+} \frac{\partial s_i^- / s^+}{\partial s_i^-} \quad (14)$$

One can verify that InfoNCE is the special case of L_{Uni} by setting $s^+ = e^{\gamma \mathbf{h}^T \mathbf{h}^+}$ and $s_i^- = e^{\gamma \mathbf{h}^T \mathbf{h}_i^-}$.

DebiasedInfoNCE [7] points out sampling from the data distribution \hat{q} will harm the model performance because the positive samples may be mistaken for negative ones. Denote $h(\cdot)$ as the labeling function, they suggest to draw negative samples from $\hat{q}_x^-(\hat{x}^-) = p(\hat{x}^- | h(\hat{x}^-) \neq h(x))$, which can be viewed as the real distribution of negative ligands. To study the event of $\{h(\hat{x}^-) \neq h(x)\}$, they further consider the joint distribution $p(\hat{x}, c) = p(\hat{x}|c)p(c)$ over data x and label c . By

assuming the class probability $p(c) = \tau^+$ as uniform, and let $\tau^- = 1 - \tau^+$ as the probability of observing any different class, they decompose \hat{q} as $\tau^- \hat{q}_x^-(x^-) + \tau^+ \hat{q}_x^+(x^-)$ and propose

$$L_{\text{Debiased}} = \mathbb{E}_{\substack{x \sim p, \hat{x}^+ \sim p_x^+, \\ \{\hat{x}_i^-\}_{i=1}^N \sim \hat{q}_x^-}} \left[\log \left(1 + \frac{Q}{N} \sum_{i=1}^N s_i^- / s^+ \right) \right] \quad (15)$$

$$(16)$$

By choosing $s^+ = e^{\mathbf{h}^T \hat{\mathbf{h}}^+}$, $s_i^- = e^{\mathbf{h}^T \hat{\mathbf{h}}_i^-}$, and replace $\hat{q}_x^-(x^-) = (\hat{q} - \tau^+ \hat{q}_x^+) / \tau^-$, with mild assumptions, the approximated debaised InfoNCE can be written as:

$$L_{\text{Debiased}} \approx \mathbb{E}_{x \sim p, x^+ \sim p_x^+} \left[\log \left(1 + \frac{1}{\tau^-} \sum_{i=1}^N (e^{\mathbf{h}^T \hat{\mathbf{h}}_i^- - \mathbf{h}^T \hat{\mathbf{h}}^+} - \tau^+) \right) \right] \quad (17)$$

ChemInfoNCE For the case of classification with discrete labels, the assumption of uniform class probabilities may be too strong, especially for the unbalanced dataset. When it comes to regression, molecules have continuous chemical properties and the event $\{h(\hat{x}) \neq h(\hat{x}^-)\}$ can not describe the validity of negative data. Considering these challenges, we introduce a new event $\{\text{score}(\hat{x}, \hat{x}^-) < \tau\}$ to measure the validity of negative samples, where $\text{score}(\cdot)$ is the function of chemical similarity. The underlying hypothesis is that molecules with lower chemical semantics are more likely to be negative samples. Thus, we define the true negative probability as:

$$q_x^-(\hat{x}^-) := q(\hat{x}^- | \text{sim}(x, \hat{x}^-) < \tau) \propto \max(1 - \text{sim}(x, \hat{x}^-) - \tau, 0) \cdot p(\hat{x}^-) \quad (18)$$

By denoting $w_i = \max(1 - \text{sim}(x, \hat{x}^-) - \tau, 0)$, similar to DebiasedInfoNCE, the final ChemInfoNCE can be simplified as:

$$L_{\text{Chem}} \approx \mathbb{E}_{x \sim p, x^+ \sim p_x^+} \left[\log \left(1 + \sum_{i=1}^N (\rho_i e^{\mathbf{h}^T \hat{\mathbf{h}}_i^- - \mathbf{h}^T \hat{\mathbf{h}}^+}) \right) \right] \quad (19)$$

where $\rho_i = \frac{w_i}{\sum_{i=1}^N w_i}$. We provide a detailed derivation in the appendix.

4 Experiments

In this section, we conduct extensive experiments to reveal the effectiveness of the proposed method from three perspectives:

1. **Pocket:** How does the pre-trained pocket model perform on the pocket matching tasks?
2. **Ligand:** Could the ligand model provide good performance in predicting molecular properties?
3. **Pocket-ligand:** Can the joint model improve the performance of finding potentially binding pocket-ligand pairs, i.e., virtual screening?

4.1 Pretraining setup

Pretraining Dataset We adopt BioLip [55] dataset for co-supervised pretraining, where the original BioLip contains 573,225 entries up to 2022.04.01. Compared to PDDBind [46] with 23,496 complexes, BioLip contains more complexes that lack binding affinity, thus could provide a more comprehensive view of binding mode analysis. To focus on the drug-like molecules and their binding pockets, we filtered out other unrelated complexes that contain pipelines, DNA, RNA, single ions, etc. The whole data preprocessing pipeline can be found in the appendix.

Experimental setting We pretrain stacked GGMPs via ChemInfoNCE loss to minimize the distance of positive pairs, while maximizing the distance of negative pairs. Experiments are conducted on NVIDIA A100s, where the learning rate is 0.01 and the batch size is 100.

4.2 Downstream task 1: Pocket matching

Experimental setup Could the pre-trained model identify chemically similar pockets from various pockets? We explore the discriminative ability of the pocket model with the pocket matching tasks. To comprehensively understand the potential of the proposed method, we evaluated it on 10 benchmarks recently collected in the ProSPECCTs dataset [12]. For each benchmark, the positive and negative pairs of pockets are defined differently according to the research objectives. We summarize 5 research objectives as **O1**: Whether the model is robust to the pocket definition? **O2**: Whether the model is robust to the pocket flexibility? **O3**: Can the model distinguish between pockets with different properties? **O4**: Whether the model can distinguish dissimilar proteins binding to identical ligands and cofactors? **O5**: How about the performance on real applications? The motivation and dataset descriptions of these objectives can be found in Table. 2. We report the AUC-ROC scores on all benchmarks.

Name	Goal	Description	$\frac{N_{pos}}{N_{neg}}$
D1	Pocket definition.	D1 contains structures with identical sequences. Since the same pocket could bind to different ligands, diverse pocket definition will influence the learned representations.	13430/92846
D1.2	Impact of ligand diversity.	D1.2 is a reduced set of D1 that exclusively contains structures with identical sequences and similar ligands.	241/1784
D2	Conformational flexibility.	D2 uses NMR structures that provide conformational ensembles of protein structures, where the same pockets contain larger and smaller conformational variations.	7729/100512
D3	Physicochemical properties	Based on D1, D3 further adds negative samples by replacing pockets’ residues with ones that have different physicochemical properties and similar size.	13430/67150
D4	Physicochemical and shape properties.	Based on D1, D3 further adds negative samples by replacing pockets’ residues with ones whose number of carbon and hetero atoms differs by at least three atoms.	13430/67150
D5	Impact of binding site features, interaction patterns	Kahraman data set without phosphate binding sites	920/5480
D5.2	Similar to D5.	Kahraman data set	1,320/8,680
D6	Relationships between pockets binding to identical ligands.	Barelier data set	19/43
D6.2	Similar to D6.	Barelier data set including cofactors	19/43
D7	Successful applications	D7 consists of pocket pairs which were previously characterized as being similar in published literature	115/56284

Table 2: Pocket matching benchmarks and objectives.

Baselines We compare the proposed approach with both classical and deep learning baselines. The classical methods can be divided into profile-based, graph-based and grid-based ones. The profile-based methods encode topological, physicochemical and statistical properties in a unified way for comparing various pockets, e.g., SiteAlign [35], RAPMAD [22], TIFP [10], FuzCav [49], PocketMatch[59], SMAP[53], TM-align[62], KRIPO[51] and Grim [10]. The graph-based methods adopt isomorphism detection algorithm to find the common motifs between pockets, e.g., Cavbase [36], IsoMIF[6], ProBiS[21]. Grid-based methods represent protein pockets by regularly spaced pharmacophoric grid points, e.g., VolSite/Shaper [9]. Another tools such as SiteEngines[38] and SiteHopper[2] are also included. As to deep learning approaches, we compare with the recent SOTA algorithm–DeeplyTough[39].

Results and analyses We present the pocket matching results in Table. 3, where the pretrained model achieves competitive results in most cases. Specifically, CoSP is robust to pocket definition (**O1**) and achieves the highest AUC scores in D1 and D1.2. The robustness also remains when

considering conformational variability (**O2**), where CoSP achieves 0.99 AUC score in D2. It should be noted that robustness to homogeneous pockets does not mean that the model has poor discrimination; on the contrary, the model could identify pockets with different physicochemical and shape properties (**O3**) in D3 and D4. Compared with previous deep learning methods (DeeplyTough), CoSP provides better performance in distinguishing different pockets bound to the same ligands and cofactors (**Q4**), refer to the results of D5, D5.2, D6 and D6.2. Last but not least, CoSP showed good potential for practical applications (**O5**) with 0.81 AUC score.

	D1	D1.2	D2	D3	D4	D5	D5.2	D6	D6.2	D7
Cavbase	0.98	0.91	0.87	0.65	0.64	0.60	0.57	0.55	0.55	0.82
FuzCav	0.94	0.99	0.99	0.69	0.58	0.55	0.54	0.67	0.73	0.77
FuzCav (PDB)	0.94	0.99	0.98	0.69	0.58	0.56	0.54	0.65	0.72	0.77
grim	0.69	0.97	0.92	0.55	0.56	0.69	0.61	0.45	0.65	0.70
grim (PDB)	0.62	0.83	0.85	0.57	0.56	0.61	0.58	0.45	0.50	0.64
IsoMIF	0.77	0.97	0.70	0.59	0.59	0.75	0.81	0.62	0.62	0.87
KRIPO	0.91	1.00	0.96	0.60	0.61	0.76	0.77	0.73	0.74	0.85
PocketMatch	0.82	0.98	0.96	0.59	0.57	0.66	0.60	0.51	0.51	0.82
ProBiS	1.00	1.00	1.00	0.47	0.46	0.54	0.55	0.50	0.50	0.85
RAPMAD	0.85	0.83	0.82	0.61	0.63	0.55	0.52	0.60	0.60	0.74
shaper	0.96	0.93	0.93	0.71	0.76	0.65	0.65	0.54	0.65	0.75
shaper (PDB)	0.96	0.93	0.93	0.71	0.76	0.66	0.64	0.54	0.65	0.75
VolSite/shaper	0.93	0.99	0.78	0.68	0.76	0.56	0.58	0.71	0.76	0.77
VolSite/shaper (PDB)	0.94	1.00	0.76	0.68	0.76	0.57	0.56	0.50	0.57	0.72
SiteAlign	0.97	1.00	1.00	0.85	0.80	0.59	0.57	0.44	0.56	0.87
SiteEngine	0.96	1.00	1.00	0.82	0.79	0.64	0.57	0.55	0.55	0.86
SiteHopper	0.98	0.94	1.00	0.75	0.75	0.72	0.81	0.56	0.54	0.77
SMAP	1.00	1.00	1.00	0.76	0.65	0.62	0.54	0.68	0.68	0.86
TIFP	0.66	0.90	0.91	0.66	0.66	0.71	0.63	0.55	0.60	0.71
TIFP (PDB)	0.55	0.74	0.78	0.56	0.57	0.54	0.53	0.56	0.61	0.66
TM-align	1.00	1.00	1.00	0.49	0.49	0.66	0.62	0.59	0.59	0.88
DeeplyTough	0.95	0.98	0.90	0.76	0.75	0.67	0.63	0.54	0.54	0.83
CoSP	1.00	1.00	0.99	0.79	0.81	0.62	0.63	0.61	0.62	0.81

Table 3: Pocket matching results.

4.3 Downstream task 2: Molecule property prediction

Experimental setup Could the model learn expressive features for molecule classification and regression tasks? We evaluate CoSP on 9 benchmarks collected by MoleculeNet[52]. Following previous researches, we use scaffold splitting to generate train/validation/test set with a ratio of 8:1:1. We report AUC-ROC and RMSE metrics for classification and regression tasks, respectively. The mean and standard deviations of results over three random seeds are provided by default.

Methods	Classification (AUC-ROC % \uparrow)						Regression (RMSE \downarrow)		
	BBBP	BACE	ClinTox	Tox21	ToxCast	SIDER	ESOL	FreeSolv	Lipo
Dataset	2039	1513	1478	7831	8575	1427	1128	642	4200
#Molecules	1	1	2	12	617	27	1	1	1
#Tasks	1	1	2	12	617	27	1	1	1
D-MPNN	71.0(0.3)	80.9(0.6)	90.6(0.6)	75.9(0.7)	65.5(0.3)	57.0(0.7)	1.050(0.008)	2.082(0.082)	0.683(0.016)
Attentive FP	64.3(1.8)	78.4(0.02)	84.7(0.3)	76.1(0.5)	63.7(0.2)	60.6(3.2)	0.877(0.029)	2.073(0.183)	0.721(0.001)
N-Gram _{RF}	69.7(0.6)	77.9(1.5)	77.5(4.0)	74.3(0.4)	—	66.8(0.7)	1.074(0.107)	2.688(0.085)	0.812(0.028)
N-Gram _{XGB}	69.1(0.8)	79.1(1.3)	87.5(2.7)	75.8(0.9)	—	65.5(0.7)	1.083(0.082)	5.061(0.744)	2.072(0.030)
MolCLR	72.2(2.1)	82.4(0.9)	91.2(3.5)	75.0(0.2)	—	58.9(1.4)	1.271(0.040)	2.594(0.249)	0.691(0.004)
PretrainGNN	68.7(1.3)	84.5(0.7)	72.6(1.5)	78.1(0.6)	65.7(0.6)	62.7(0.8)	1.100(0.006)	2.764(0.002)	0.739(0.003)
GraphMVP-G	70.8(0.5)	79.3(1.5)	79.1(2.8)	75.9(0.5)	63.1(0.2)	60.2(1.1)	—	—	—
GraphMVP-C	72.4(1.6)	81.2(0.9)	76.3(1.9)	74.4(0.2)	63.1(0.4)	63.9(1.2)	—	—	—
3DInfomax	69.1(1.1)	79.4(1.9)	59.4(3.2)	74.5(0.7)	64.4(0.9)	53.4(3.3)	0.894(0.028)	2.34(0.227)	0.695(0.012)
MICRO-graph	77.2(2.0)	84.4(1.1)	77.0(2.0)	77.0(0.8)	65.2(0.8)	56.7(1.1)	—	—	—
GROVER _{base}	70.0(0.1)	82.6(0.7)	81.2(3.0)	74.3(0.1)	65.4(0.4)	64.8(0.6)	0.983(0.090)	2.176(0.052)	0.817(0.008)
GROVER _{large}	69.5(0.1)	81.0(1.4)	76.2(3.7)	73.5(0.1)	65.3(0.5)	65.4(0.1)	0.895(0.017)	2.272(0.051)	0.823(0.010)
GEM	72.4(0.4)	85.6(1.1)	90.1(1.3)	78.1(0.1)	69.2(0.4)	67.2(0.4)	0.798(0.029)	1.877(0.094)	0.660(0.008)
Uni-Mol	72.9(0.6)	85.7(0.2)	91.9(1.8)	79.6(0.5)	69.6(0.1)	65.9(1.3)	0.788(0.029)	1.620(0.035)	0.603(0.010)
CoSP	73.1(0.3)	84.3(1.1)	91.3(1.5)	78.5(0.1)	69.3(0.2)	64.7(1.5)	0.785(0.029)	1.752(0.042)	0.621(0.012)

Table 4: Molecule property prediction

Baselines We evaluate CoSP against 14 baselines, including D-MPNN [56], Attentive FP [54], N-Gram_{RF}, N-Gram_{XGB} [24], MolCLR [47], PretrainGNN [19], GraphMVP-G, GraphMVP-C [26], 3DInfomax [40], MICRO-graph [61], GROVER_{base}, GROVER_{large} [33], GEM [13] and Uni-Mol [65]. Except for N-Gram_{RF} and N-Gram_{XGB}, all these baselines are pretraining methods. Some of the methods mentioned in the related works are not included because the experimental setup, e.g., data splitting, may be different.

Results and analysis We show results in Table.4. The main observations are: (1) CoSP could not achieve the best results, probably because we used much less pre-training data than baseline methods. However, we have used complex data we could find, and more data will take a long time to accumulate. (2) CoSP achieves competitive results on both classification and regression and outperforms most of the baselines. These results indicate that the model could learn expressive molecular features for property prediction. With the increasing amount of complexes, we believe that the performance can be further improved.

4.4 Downstream task 3: Virtual screening

Experimental setup Could the model distinguish molecules most likely to bind to the protein pockets? We evaluate CoSP on the DUD-E [28] dataset which consists of 102 targets across different protein families. For each target, DUD-E provides 224 actives (positive examples) and 10,000 decoy ligands (negative examples) in average. The decoys were calculated by choosing them to be physically similar but topologically different from the actives. During finetuning, we use the same data splitting as GraphCNN [44], and report the AUC-ROC and ROC enrichment (RE) scores. Note that $x\%$ RE indicates the ratio of the true positive rate (TPR) to the false positive rate (FPR) at $x\%$ FPR value.

Baselines We compare CoSP with AutoDock Vina [45], RF-score [1], NNScore [11], 3DCNN [31] and GraphCNN [44]. AutoDock Vina is a commonly used open-source program for doing molecular docking. RF-score uses random forest to capture protein-ligand binding effects. NNScore, 3DCNN, and GraphCNN use MLP, CNN and GNN to learn the protein-ligand binding, respectively.

	AUC-ROC \uparrow	0.5% RE \uparrow	DUD-E		
			1.0% RE \uparrow	2.0% RE \uparrow	5.0% RE \uparrow
Vina	0.716	9.139	7.321	5.881	4.444
RF-score	0.622	5.628	4.274	3.499	2.678
NNScore	0.584	4.166	2.980	2.460	1.891
Graph CNN	0.886	44.406	29.748	19.408	10.735
3DCNN	0.868	42.559	29.654	19.363	10.710
CoSP	0.901	51.048	35.978	23.681	12.212

Table 5: Virtual screening results on DUD-E

Results and analysis We present results in Table.5, and observe that: (1) Random forest and MLP-based RF-score and NNScore achieve competitive results to Vina, indicating the potential of machine learning in virtual screening. (2) Deep learning-based Graph CNN and 3DCNN significantly outperform both RF-score and NNScore. (3) CoSP provides the best results by achieving a 0.90 AUC score and outperforms baselines in RE scores.

5 Conclusion

This paper proposes a co-supervised pretraining framework to learn pocket and ligand spaces via contrastive learning jointly. The pretrained model could achieve competitive results on pocket matching, molecule property predictions, and virtual screening by injecting the interaction knowledge. We hope the unified modeling framework could further boost the development of AI drug discovery.

References

- [1] Pedro J Ballester and John BO Mitchell. A machine learning approach to predicting protein–ligand binding affinity with applications to molecular docking. *Bioinformatics*, 26(9):1169–1175, 2010.
- [2] Jose Batista, Paul CD Hawkins, Robert Tolbert, and Matthew T Geballe. Sitehopper-a unique tool for binding site comparison. *Journal of Cheminformatics*, 6(1):1–1, 2014.
- [3] Simon Batzner, Albert Musaelian, Lixin Sun, Mario Geiger, Jonathan P Mailoa, Mordechai Kornbluth, Nicola Molinari, Tess E Smidt, and Boris Kozinsky. E (3)-equivariant graph neural networks for data-efficient and accurate interatomic potentials. *Nature communications*, 13(1):1–11, 2022.
- [4] Johannes Brandstetter, Rob Hesselink, Elise van der Pol, Erik Bekkers, and Max Welling. Geometric and physical quantities improve e (3) equivariant message passing. *arXiv preprint arXiv:2110.02905*, 2021.
- [5] Nigel Chaffey. Alberts, b., johnson, a., lewis, j., raff, m., roberts, k. and walter, p. molecular biology of the cell. 4th edn., 2003.
- [6] Matthieu Chartier and Rafael Najmanovich. Detection of binding site molecular interaction field similarities. *Journal of chemical information and modeling*, 55(8):1600–1615, 2015.
- [7] Ching-Yao Chuang, Joshua Robinson, Yen-Chen Lin, Antonio Torralba, and Stefanie Jegelka. Debaised contrastive learning. *Advances in neural information processing systems*, 33:8765–8775, 2020.
- [8] Taco Cohen and Max Welling. Group equivariant convolutional networks. In *International conference on machine learning*, pages 2990–2999. PMLR, 2016.
- [9] Jérémy Desaphy, Karima Azdimousa, Esther Kellenberger, and Didier Rognan. Comparison and druggability prediction of protein–ligand binding sites from pharmacophore-annotated cavity shapes, 2012.
- [10] Jeremy Desaphy, Eric Raimbaud, Pierre Ducrot, and Didier Rognan. Encoding protein–ligand interaction patterns in fingerprints and graphs. *Journal of chemical information and modeling*, 53(3):623–637, 2013.
- [11] Jacob D Durrant and J Andrew McCammon. Nnscore: a neural-network-based scoring function for the characterization of protein- ligand complexes. *Journal of chemical information and modeling*, 50(10):1865–1871, 2010.
- [12] Christiane Ehrt, Tobias Brinkjost, and Oliver Koch. A benchmark driven guide to binding site comparison: An exhaustive evaluation using tailor-made data sets (prospeccts). *PLoS computational biology*, 14(11):e1006483, 2018.
- [13] Xiaomin Fang, Lihang Liu, Jieqiong Lei, Donglong He, Shanzhuo Zhang, Jingbo Zhou, Fan Wang, Hua Wu, and Haifeng Wang. Geometry-enhanced molecular representation learning for property prediction. *Nature Machine Intelligence*, 4(2):127–134, 2022.
- [14] Yin Fang, Haihong Yang, Xiang Zhuang, Xin Shao, Xiaohui Fan, and Huajun Chen. Knowledge-aware contrastive molecular graph learning. *arXiv preprint arXiv:2103.13047*, 2021.
- [15] Fabian Fuchs, Daniel Worrall, Volker Fischer, and Max Welling. Se (3)-transformers: 3d roto-translation equivariant attention networks. *Advances in Neural Information Processing Systems*, 33:1970–1981, 2020.
- [16] Octavian-Eugen Ganea, Xinyuan Huang, Charlotte Bunne, Yatao Bian, Regina Barzilay, Tommi Jaakkola, and Andreas Krause. Independent se (3)-equivariant models for end-to-end rigid protein docking. *arXiv preprint arXiv:2111.07786*, 2021.
- [17] Zhangyang Gao, Cheng Tan, Stan Li, et al. Alphadesign: A graph protein design method and benchmark on alphafolddb. *arXiv preprint arXiv:2202.01079*, 2022.

- [18] Jiaqi Guan, Wesley Wei Qian, Wei-Ying Ma, Jianzhu Ma, Jian Peng, et al. Energy-inspired molecular conformation optimization. In *International Conference on Learning Representations*, 2021.
- [19] Weihua Hu, Bowen Liu, Joseph Gomes, Marinka Zitnik, Percy Liang, Vijay Pande, and Jure Leskovec. Strategies for pre-training graph neural networks. *arXiv preprint arXiv:1905.12265*, 2019.
- [20] Sarah L Kinnings, Nina Liu, Nancy Buchmeier, Peter J Tonge, Lei Xie, and Philip E Bourne. Drug discovery using chemical systems biology: repositioning the safe medicine comtan to treat multi-drug and extensively drug resistant tuberculosis. *PLoS computational biology*, 5(7):e1000423, 2009.
- [21] Janez Konc and Dušanka Janežič. Probis algorithm for detection of structurally similar protein binding sites by local structural alignment. *Bioinformatics*, 26(9):1160–1168, 2010.
- [22] Timo Krotzky, Christian Grunwald, Ute Egerland, and Gerhard Klebe. Large-scale mining for similar protein binding pockets: with rapmad retrieval on the fly becomes real. *Journal of chemical information and modeling*, 55(1):165–179, 2015.
- [23] Pengyong Li, Jun Wang, Yixuan Qiao, Hao Chen, Yihuan Yu, Xiaojun Yao, Peng Gao, Guotong Xie, and Sen Song. An effective self-supervised framework for learning expressive molecular global representations to drug discovery. *Briefings in Bioinformatics*, 22(6):bbab109, 2021.
- [24] Shengchao Liu, Mehmet F Demirel, and Yingyu Liang. N-gram graph: Simple unsupervised representation for graphs, with applications to molecules. *Advances in neural information processing systems*, 32, 2019.
- [25] Shengchao Liu, Hanchen Wang, Weiyang Liu, Joan Lasenby, Hongyu Guo, and Jian Tang. Pre-training molecular graph representation with 3d geometry—rethinking self-supervised learning on structured data.
- [26] Shengchao Liu, Hanchen Wang, Weiyang Liu, Joan Lasenby, Hongyu Guo, and Jian Tang. Pre-training molecular graph representation with 3d geometry. *arXiv preprint arXiv:2110.07728*, 2021.
- [27] Amy X Lu, Haoran Zhang, Marzyeh Ghassemi, and Alan Moses. Self-supervised contrastive learning of protein representations by mutual information maximization. *BioRxiv*, 2020.
- [28] Michael M Mysinger, Michael Carchia, John J Irwin, and Brian K Shoichet. Directory of useful decoys, enhanced (dud-e): better ligands and decoys for better benchmarking. *Journal of medicinal chemistry*, 55(14):6582–6594, 2012.
- [29] Thin Nguyen, Hang Le, Thomas P Quinn, Tri Nguyen, Thuc Duy Le, and Svetha Venkatesh. Graphdta: Predicting drug–target binding affinity with graph neural networks. *Bioinformatics*, 37(8):1140–1147, 2021.
- [30] Aaron van den Oord, Yazhe Li, and Oriol Vinyals. Representation learning with contrastive predictive coding. *arXiv preprint arXiv:1807.03748*, 2018.
- [31] Matthew Ragoza, Joshua Hochuli, Elisa Idrobo, Jocelyn Sunseri, and David Ryan Koes. Protein–ligand scoring with convolutional neural networks. *Journal of chemical information and modeling*, 57(4):942–957, 2017.
- [32] Joshua Robinson, Ching-Yao Chuang, Suvrit Sra, and Stefanie Jegelka. Contrastive learning with hard negative samples. *arXiv preprint arXiv:2010.04592*, 2020.
- [33] Yu Rong, Yatao Bian, Tingyang Xu, Weiyang Xie, Ying Wei, Wenbing Huang, and Junzhou Huang. Self-supervised graph transformer on large-scale molecular data. *Advances in Neural Information Processing Systems*, 33:12559–12571, 2020.
- [34] Victor Garcia Satorras, Emiel Hoogetboom, and Max Welling. E (n) equivariant graph neural networks. In *International conference on machine learning*, pages 9323–9332. PMLR, 2021.

- [35] Claire Schalon, Jean-Sébastien Surgand, Esther Kellenberger, and Didier Rognan. A simple and fuzzy method to align and compare druggable ligand-binding sites. *Proteins: Structure, Function, and Bioinformatics*, 71(4):1755–1778, 2008.
- [36] Stefan Schmitt, Daniel Kuhn, and Gerhard Klebe. A new method to detect related function among proteins independent of sequence and fold homology. *Journal of molecular biology*, 323(2):387–406, 2002.
- [37] Aditya Divyakant Shrivastava and Douglas B Kell. Fragnet, a contrastive learning-based transformer model for clustering, interpreting, visualizing, and navigating chemical space. *Molecules*, 26(7):2065, 2021.
- [38] Alexandra Shulman-Peleg, Ruth Nussinov, and Haim J Wolfson. Siteengines: recognition and comparison of binding sites and protein–protein interfaces. *Nucleic acids research*, 33(suppl_2):W337–W341, 2005.
- [39] Martin Simonovsky and Joshua Meyers. Deeplytough: learning structural comparison of protein binding sites. *Journal of chemical information and modeling*, 60(4):2356–2366, 2020.
- [40] Hannes Stärk, Dominique Beaini, Gabriele Corso, Prudencio Tossou, Christian Dallago, Stephan Günnemann, and Pietro Liò. 3d infomax improves gnns for molecular property prediction. *arXiv preprint arXiv:2110.04126*, 2021.
- [41] Pascal Sturmfels, Jesse Vig, Ali Madani, and Nazneen Fatema Rajani. Profile prediction: An alignment-based pre-training task for protein sequence models. *arXiv preprint arXiv:2012.00195*, 2020.
- [42] Mengying Sun, Jing Xing, Huijun Wang, Bin Chen, and Jiayu Zhou. Mocl: data-driven molecular fingerprint via knowledge-aware contrastive learning from molecular graph. In *Proceedings of the 27th ACM SIGKDD Conference on Knowledge Discovery & Data Mining*, pages 3585–3594, 2021.
- [43] Nathaniel Thomas, Tess Smidt, Steven Kearnes, Lusann Yang, Li Li, Kai Kohlhoff, and Patrick Riley. Tensor field networks: Rotation-and translation-equivariant neural networks for 3d point clouds. *arXiv preprint arXiv:1802.08219*, 2018.
- [44] Wen Torng and Russ B Altman. Graph convolutional neural networks for predicting drug-target interactions. *Journal of chemical information and modeling*, 59(10):4131–4149, 2019.
- [45] AutoDock Vina. Improving the speed and accuracy of docking with a new scoring function, efficient optimization, and multithreading. *J. Comput. Chem*, 31(2):455–461, 2010.
- [46] Renxiao Wang, Xueliang Fang, Yipin Lu, Chao-Yie Yang, and Shaomeng Wang. The pdbind database: methodologies and updates. *Journal of medicinal chemistry*, 48(12):4111–4119, 2005.
- [47] Yuyang Wang, Jianren Wang, Zhonglin Cao, and Amir Barati Farimani. Molecular contrastive learning of representations via graph neural networks. *Nature Machine Intelligence*, 4(3):279–287, 2022.
- [48] Alexander Weber, Angela Casini, Andreas Heine, Daniel Kuhn, Claudiu T Supuran, Andrea Scozzafava, and Gerhard Klebe. Unexpected nanomolar inhibition of carbonic anhydrase by cox-2-selective celecoxib: new pharmacological opportunities due to related binding site recognition. *Journal of medicinal chemistry*, 47(3):550–557, 2004.
- [49] Nathanaël Weill and Didier Rognan. Alignment-free ultra-high-throughput comparison of drug-gable protein- ligand binding sites. *Journal of chemical information and modeling*, 50(1):123–135, 2010.
- [50] Dominica Willmann, Soyoung Lim, Stefan Wetzel, Eric Metzger, Anett Jandausch, Wolfram Wilk, Manfred Jung, Ignasi Forne, Axel Imhof, Andreas Janzer, et al. Impairment of prostate cancer cell growth by a selective and reversible lysine-specific demethylase 1 inhibitor. *International Journal of Cancer*, 131(11):2704–2709, 2012.

- [51] David J Wood, Jacob de Vlieg, Markus Wagener, and Tina Ritschel. Pharmacophore fingerprint-based approach to binding site subpocket similarity and its application to bioisostere replacement. *Journal of chemical information and modeling*, 52(8):2031–2043, 2012.
- [52] Zhenqin Wu, Bharath Ramsundar, Evan N Feinberg, Joseph Gomes, Caleb Geniesse, Aneesh S Pappu, Karl Leswing, and Vijay Pande. Moleculenet: a benchmark for molecular machine learning. *Chemical science*, 9(2):513–530, 2018.
- [53] Lei Xie and Philip E Bourne. Detecting evolutionary relationships across existing fold space, using sequence order-independent profile–profile alignments. *Proceedings of the National Academy of sciences*, 105(14):5441–5446, 2008.
- [54] Zhaoping Xiong, Dingyan Wang, Xiaohong Liu, Feisheng Zhong, Xiaozhe Wan, Xutong Li, Zhaojun Li, Xiaomin Luo, Kaixian Chen, Hualiang Jiang, et al. Pushing the boundaries of molecular representation for drug discovery with the graph attention mechanism. *Journal of medicinal chemistry*, 63(16):8749–8760, 2019.
- [55] Jianyi Yang, Ambrish Roy, and Yang Zhang. Biolip: a semi-manually curated database for biologically relevant ligand–protein interactions. *Nucleic acids research*, 41(D1):D1096–D1103, 2012.
- [56] Kevin Yang, Kyle Swanson, Wengong Jin, Connor Coley, Philipp Eiden, Hua Gao, Angel Guzman-Perez, Timothy Hopper, Brian Kelley, Miriam Mathea, et al. Analyzing learned molecular representations for property prediction. *Journal of chemical information and modeling*, 59(8):3370–3388, 2019.
- [57] Kevin K Yang, Alex Xijie Lu, and Nicolo Fusi. Convolutions are competitive with transformers for protein sequence pretraining. In *ICLR2022 Machine Learning for Drug Discovery*, 2022.
- [58] Yongliang Yang, Guohui Li, Dongyu Zhao, Haoyang Yu, Xiliang Zheng, Xiangda Peng, Xiaoe Zhang, Ting Fu, Xiaoqing Hu, Mingshan Niu, et al. Computational discovery and experimental verification of tyrosine kinase inhibitor pazopanib for the reversal of memory and cognitive deficits in rat model neurodegeneration. *Chemical science*, 6(5):2812–2821, 2015.
- [59] Kalidas Yeturu and Nagasuma Chandra. Pocketmatch: a new algorithm to compare binding sites in protein structures. *BMC bioinformatics*, 9(1):1–17, 2008.
- [60] Ningyu Zhang, Zhen Bi, Xiaozhuan Liang, Siyuan Cheng, Haosen Hong, Shumin Deng, Jiazhang Lian, Qiang Zhang, and Huajun Chen. Ontoprotein: Protein pretraining with gene ontology embedding. *arXiv preprint arXiv:2201.11147*, 2022.
- [61] Shichang Zhang, Ziniu Hu, Arjun Subramonian, and Yizhou Sun. Motif-driven contrastive learning of graph representations. *arXiv preprint arXiv:2012.12533*, 2020.
- [62] Yang Zhang and Jeffrey Skolnick. Tm-align: a protein structure alignment algorithm based on the tm-score. *Nucleic acids research*, 33(7):2302–2309, 2005.
- [63] Zaixi Zhang, Qi Liu, Hao Wang, Chengqiang Lu, and Chee-Kong Lee. Motif-based graph self-supervised learning for molecular property prediction. *Advances in Neural Information Processing Systems*, 34:15870–15882, 2021.
- [64] Zuobai Zhang, Minghao Xu, Arian Jamasb, Vijil Chenthamarakshan, Aurelie Lozano, Payel Das, and Jian Tang. Protein representation learning by geometric structure pretraining. *arXiv preprint arXiv:2203.06125*, 2022.
- [65] Gengmo Zhou, Zhifeng Gao, Qiankun Ding, Hang Zheng, Hongteng Xu, Zhewei Wei, Linfeng Zhang, and Guolin Ke. Uni-mol: A universal 3d molecular representation learning framework. 2022.